

compound $K[NEt_4][Co^{II}(SC_{10}H_{13})_4]$. The reaction of 2 equiv of $LiSC_{10}H_{13}$ with $CoCl_2$ in ethanol or CH_3CN gives a light green precipitate whose elemental analysis is consistent with a $Co(SC_{10}H_{13})_2$ formulation.¹⁴ This compound is insoluble in alcohols, CH_3CN , hexane, and toluene but is soluble in DMF to give blue-green solutions.

The average Co-S bond length in **1** (2.28 (1) Å) is 0.03 Å shorter than the corresponding distance in $[PPh_4]_2[Co(SPh)_4]$.¹³ The difference in the overall charge on the anions is principally responsible for the discrepancy in these parameters.^{2,3} Also, the differences in the Co-S-Ph conformation may contribute to the change in the bond distances. In **1** the Co-S bonds are approximately orthogonal to plane of the durene ring, while in $Co(SPh)_4^{2-}$ the Co-S bonds lie in the plane determined by the phenyl rings.¹³ The bond angles of the CoS_3N unit show large deviations from the normal tetrahedral angle of 109.5°; these deviations result from the mixed-ligand coordination and the steric interactions among the ligands.

White crystals of $[N(n-Pr)_4][Cu(SC_{10}H_{13})_2]$ (**2**) are obtained in 60% yield from the cooled filtrate of the room-temperature reaction of 1 equiv of $Cu(CH_3CN)_4BF_4$ and $[N(n-Pr)_4]Br$ with 3 equiv of $LiSC_{10}H_{13}$ in ethanol. The linear digonal coordination of the copper was revealed by an X-ray crystal structure determination (Figure 2).¹⁵ The anion has crystallographic C_2 symmetry with the S-Cu-S' angle equal to 178.6 (1)°. The Cu-S distance of 2.137 (2) Å is substantially shorter than the average Cu-S distance in the three-coordinate copper in $[Ph_4P]_2[Cu(SPh)_3]$ ⁸ and slightly less than average Cu-S distance for the two-coordinate coppers in $[Cu_5(SPh)_7]^{2-}$ and $[Cu_5(S-t-Bu)_6]^{-,9,10}$. The observed large change in the Cu-S distance as a function of coordination number should be a valuable consideration in the interpretation of EXAFS data of copper proteins.¹⁶

A benzenethiolate complex, $(PPh_4)[Cu(SPh)_2]$, which is analogous to **2**, was previously reported but was not structurally characterized.⁸ $[Cu(SPh)_2]^-$ differs from **2** in that it readily undergoes oligomerization reactions to give the cluster compounds $[Cu_4(SPh)_6]^{2-}$ and $[Cu_5(SPh)_7]^{2-,8,9,11}$. The reaction of Cu(I) salts with $C_{10}H_{13}S^-$ was studied for a variety of Cu/SR ratios (5/1 to 1.5/1) and under different reaction conditions; **2** was the only isolated product, and in no case was the yellow color, which is characteristic of many $Cu^I_x(SR)_y$ cluster complexes,⁸⁻¹¹ ever detected.

The reduced tendency of 2,3,5,6-tetramethylbenzenethiolate to bridge metal centers makes it an attractive ligand for the synthesis and study of monomeric metal thiolate complexes in cases where less sterically demanding ligands give clusters or polymeric compounds.^{17,18}

Acknowledgment. This work was supported by grants provided by the donors of the Petroleum Research Fund, administered by the American Chemical Society, to S.A.K. and the National Institutes of Health (Grant No. GM 3252601) to M.M.

Registry No. **1**, 88157-99-7; **2**, 88158-01-4.

- (14) Anal. Calcd for $CoS_2C_{20}H_{26}$: C, 61.68; H, 6.73; S, 16.46. Found: C, 60.15; H, 6.74; S, 15.99.
- (15) $[N(CH_2CH_2CH_3)_4][Cu(SC_{10}H_{13})_2]$ crystallizes in the monoclinic space group $C2/c$ with $a = 10.763$ (4) Å, $b = 15.035$ (7) Å, $c = 21.176$ (4) Å, $\beta = 98.45$ (2)°, $V = 3390$ (3) Å³, and $Z = 4$. Final least-squares refinement gave $R = 0.060$ and $R_w = 0.085$ for 1140 unique reflections with $I > 3\sigma(I)$. The corresponding silver complex, $[NPr_4][Ag(SC_{10}H_{13})_2]$, is isomorphous with $a = 10.803$ (4) Å, $b = 14.997$ (9) Å, $c = 21.212$ (3) Å, $\beta = 97.92$ (2)°, and $V = 3404$ Å³.
- (16) Bordas, J.; Koch, M. H. J.; Hartmann, H.-J.; Weser, U. *FEBS Lett.* **1982**, *140*, 19-21.
- (17) Millar, M.; Lee, J. F.; Koch, S. A.; Fikar, R. *Inorg. Chem.* **1982**, *21*, 4105-4106.
- (18) Koch, S. A.; Millar, M. *J. Am. Chem. Soc.* **1983**, *105*, 3362-3363.

Supplementary Material Available: Tables of fractional coordinates and thermal parameters (3 pages). Ordering information is given on any current masthead page.

Department of Chemistry
State University of New York at Stony
Brook
Stony Brook, New York 11794

Stephen A. Koch*
Ronald Fikar

Department of Chemistry
New York University
New York, New York 10003

Michelle Millar*
Timothy O'Sullivan

Received June 15, 1983

Neutron Diffraction Analysis of $[H_3Pt_2(Ph_2PCH_2CH_2PPh_2)_2]^+[BPh_4]^-$: An Unusual Example of an Unsymmetrical $[P_2Pt(\mu-H)_2PtP_2H]$ Core

Sir:

Binuclear platinum hydride complexes of the type $[H_3Pt_2L_4]^+$ (L = tertiary phosphine) have been actively investigated in the last few years.¹⁻⁴ Interest arose in part from the easy displacement of dihydrogen by two-electron ligands⁵ such as CO, CNR, or phosphine, a displacement which in some cases is reversible.⁶ Specific examples of $[H_3Pt_2L_4]^+$ systems investigated to date include the bridging bis(phosphine) complexes of Puddephatt and co-workers¹ ($L_2 = Ph_2PCH_2PPh_2$ (dppm)), the monodentate phosphine complexes of Venanzi and his group³ ($L = PEt_3, PPh_3, PCy_3$), and the chelating bis(phosphine) complexes of Otsuka et al.⁴ ($L_2 = (t-Bu)_2PCH_2CH_2CH_2P(t-Bu)_2$ (dbpp)) and ourselves² ($L_2 = Ph_2PCH_2CH_2PPh_2$ (dppe)). The first geometry observed for the $[H_3Pt_2L_4]^+$ unit was a symmetrical one (i.e., $[HL_2Pt(\mu-H)PtL_2H]^+$), as found in a crystal structure determination carried out by Ibers, Otsuka, and co-workers.⁴ Subsequently, however, Venanzi et al. showed that the nonfluxional monodentate phosphine complexes $[H_3Pt_2(PR_3)_4]^+$ (R = ethyl, phenyl, cyclohexyl) had ¹H NMR spectra inconsistent with a symmetrical structure, and they proposed for the first time an unsymmetrical geometry (i.e., $[L_2Pt(\mu-H)_2PtL_2H]^+$) for the above compounds;^{3a} this was later confirmed by an X-ray analysis.^{3b} The unsymmetrical species was also mentioned as a possible intermediate in the interconversion of the fluxional molecule $[H_3Pt_2(dbpp)_2]^+$.⁴ In an earlier publication,^{2b} some of us reported (with H. D. Kaesz and C. B. Knobler) the synthesis and X-ray structure of $[H_3Pt_2(dppe)_2]^+$, which in-

- (1) Brown, M. P.; Puddephatt, R. J.; Rashidi, M.; Seddon, K. R. *J. Chem. Soc., Dalton Trans.* **1978**, 516; *Inorg. Chim. Acta* **1977**, *23*, L27.
- (2) (a) Minghetti, G.; Banditelli, G.; Bandini, A. L. *J. Organomet. Chem.* **1977**, *139*, C80. (b) Knobler, C. B.; Kaesz, H. D.; Minghetti, G.; Bandini, A. L.; Banditelli, G.; Bonati, F. *Inorg. Chem.* **1983**, *22*, 2324.
- (3) (a) Bracher, G.; Grove, D. M.; Pregosin, P.; Venanzi, L. M. *Angew. Chem., Int. Ed. Engl.* **1979**, *18*, 155. (b) Bachechi, F.; Bracher, G.; Grove, D. M.; Kellenberger, B.; Pregosin, P. S.; Venanzi, L. M. *Inorg. Chem.* **1983**, *22*, 1031. (c) Venanzi, L. M. *Coord. Chem. Rev.* **1982**, *43*, 251.
- (4) Tulip, T. H.; Yamagata, T.; Yoshida, T.; Wilson, R. D.; Ibers, J. A.; Otsuka, S. *Inorg. Chem.* **1979**, *18*, 2239.
- (5) (a) Minghetti, G.; Bandini, A. L.; Banditelli, G.; Bonati, F. *J. Organomet. Chem.* **1979**, *179*, C13. (b) Minghetti, G.; Bandini, A. L.; Banditelli, G.; Bonati, F.; Szostak, R.; Strouse, C. E.; Knobler, C. B.; Kaesz, H. D. *Inorg. Chem.* **1983**, *22*, 2332. (c) Brown, M. P.; Fisher, J. R.; Mills, A. J.; Puddephatt, R. J.; Thomson, M. *Inorg. Chim. Acta* **1980**, *44*, L271.
- (6) Hill, R. H.; Puddephatt, R. J. *Inorg. Chim. Acta* **1981**, *54*, L277.

Table I. Distances and Angles of the $H_3Pt_2P_4$ Core in $[H_3Pt_2(Ph_2PCH_2CH_2PPh_2)_2]^+[BPh_4]^-$

(A) Distances (Å)			
Pt(1)···Pt(2)	2.711 (1)	H(b1)···H(b2)	2.399 (3)
Pt(1)–H(t)	1.610 (2)	Pt(2)–H(b1)	1.691 (2)
Pt(1)–H(b1)	1.860 (2)	Pt(2)–H(b2)	1.656 (2)
Pt(1)–H(b2)	2.049 (2)	Pt(2)–P(3)	2.278 (1)
Pt(1)–P(1)	2.312 (1)	Pt(2)–P(4)	2.259 (1)
Pt(1)–P(2)	2.231 (1)		
(B) Angles (deg)			
H(b1)–Pt(1)–H(b2)	75.53 (9)	P(1)–Pt(1)–P(2)	86.14 (5)
H(t)–Pt(1)–H(b1)	87.99 (12)	Pt(1)–H(b1)–Pt(2)	99.39 (11)
H(t)–Pt(1)–H(b2)	87.26 (11)	Pt(1)–H(b2)–Pt(2)	93.41 (10)
H(t)–Pt(1)–P(1)	172.57 (9)	H(b1)–Pt(2)–H(b2)	91.55 (11)
H(t)–Pt(1)–P(2)	87.11 (9)	H(b1)–Pt(2)–P(3)	90.23 (8)
H(b1)–Pt(1)–P(1)	96.08 (8)	H(b1)–Pt(2)–P(4)	176.44 (9)
H(b1)–Pt(1)–P(2)	147.77 (8)	H(b2)–Pt(2)–P(3)	177.76 (9)
H(b2)–Pt(1)–P(1)	99.75 (8)	H(b2)–Pt(2)–P(4)	92.01 (9)
H(b2)–Pt(1)–P(2)	135.92 (7)	P(3)–Pt(2)–P(4)	86.21 (5)

dicated the unsymmetrical structure $[L_2Pt(\mu-H)_2PtL_2H]^+$. In this communication we report an accurate single-crystal neutron diffraction analysis of another crystalline modification of the same compound.

The compound $[H_3Pt_2(Ph_2PCH_2CH_2PPh_2)_2]^+[BPh_4]^-$ was prepared as described earlier.² Large crystals suitable for a neutron diffraction analysis were obtained via recrystallization from an acetone/ether mixture. Curiously, these large crystals had a different unit cell (triclinic, space group $P\bar{1}$) than the small specimens used in the earlier X-ray work^{2b} (monoclinic, space group $P2_1/n$), and thus the entire X-ray analysis had to be repeated in the triclinic system. A small fragment was carefully cleaved from a large crystal and used for the X-ray structure determination. Unit cell parameters are as follows: $a = 15.153$ (13) Å, $b = 11.422$ (13) Å, $c = 19.291$ (21) Å, $\alpha = 98.50$ (8)°, $\beta = 100.47$ (8)°, $\gamma = 97.57$ (7)°, $V = 3204$ (5) Å³, and $\rho(\text{calcd}) = 1.57$ g cm⁻³ for $Z = 2$. Data were collected with Mo K α radiation up to a $2\theta(\text{max})$ of 45° on a Nicolet/Syntex P2₁ diffractometer at room temperature. The structure was solved with the use of standard heavy-atom techniques and refined to final agreement factors⁷ of $R(F) = 0.052$ and $R_w(F) = 0.068$ for 6222 non-zero reflections ($I > 3\sigma(I)$). The non-hydrogen skeleton of the triclinic form of $[H_3Pt_2(\text{dppe})_2]^+[BPh_4]^-$ turned out to be essentially identical with that obtained from the monoclinic crystals.^{2b}

The subsequent neutron diffraction study was carried out on a crystal of volume 7.84 mm³ at the Brookhaven High Flux Beam Reactor. Data were collected up to a $2\theta(\text{max})$ of 106.3° with neutrons of wavelength 1.6113 (13) Å. The unit cell dimensions for the neutron analysis ($a = 15.019$ (2) Å, $b = 11.297$ (2) Å, $c = 19.111$ (3) Å, $\alpha = 98.766$ (8)°, $\beta = 100.484$ (6)°, $\gamma = 97.469$ (7)°, $V = 3109$ (1) Å³) are somewhat smaller than those for the X-ray work because of the low temperature (~20 K) used during neutron data collection. The non-hydrogen positions derived from the X-ray analysis were used to phase the neutron data, and a series of difference-Fourier maps subsequently revealed the positions of all the H atoms in the molecule. After least-squares refinement,⁸ the final agreement factors⁷ stood at $R(F^2) = 0.043$ and $R_w(F^2) = 0.046$ for all data (12 843 reflections). A listing of the important

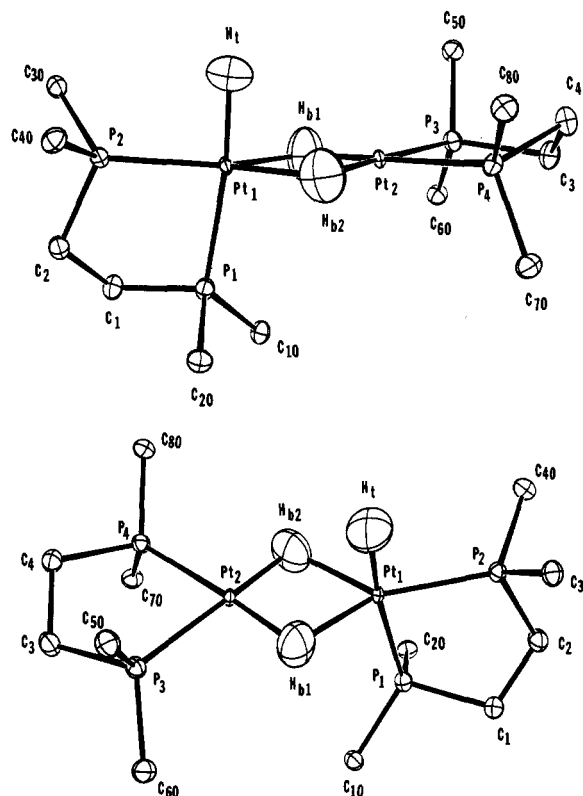


Figure 1. Two views¹⁶ of the central core of the $[H_3Pt_2(Ph_2PCH_2CH_2PPh_2)_2]^+$ cation. Only the ipso carbons of the phenyl rings are shown, for clarity.

distances and angles in the $H_3Pt_2P_4$ core is given in Table I. Complete results from the neutron analysis are available as supplementary material.

As mentioned earlier, the basic geometry of the $[H_3Pt_2(\text{dppe})_2]^+$ cation derived from the X-ray analysis^{2b} is confirmed, but with much more accurate positions for the H atoms. The structure (Figure 1) shows the unusual feature of five- and four-coordinate Pt atoms linked via two bridging H atoms. The five-coordinate platinum atom (Pt(1)) has a distorted-trigonal-bipyramidal geometry, with H(t) and P(1) as the axial atoms and P(2), H(b1), and H(b2) defining the equatorial plane ($H(b1)–Pt(1)–H(b2) = 75.5$ (1)°, $H(b1)–Pt(1)–P(2) = 147.8$ (1)°, $H(b2)–Pt(1)–P(2) = 135.9$ (1)°). The four-coordinate platinum atom (Pt(2)), on the other hand, has a normal square-planar geometry, with interatomic angles close to ideal values (Table I). The P(1)–Pt(1)–P(2) plane is approximately perpendicular to the P(3)–Pt(2)–P(4) plane.

The most noticeable feature about the two bridging H atoms is the marked asymmetry of their positions. The distances of these two atoms to Pt(2) (1.691 (2) Å, 1.656 (2) Å) are very much shorter than the corresponding distances to Pt(1) (1.860 (2) Å, 2.049 (2) Å), clearly indicating that they are interacting much more strongly with Pt(2) than with Pt(1).⁹ In fact, the H(b1)–Pt(2) and H(b2)–Pt(2) bond lengths are not much longer than the terminal Pt(1)–H(t) distance of 1.610 (2) Å, suggesting that H(b1) and H(b2) are more "terminal" in nature than "bridging". This reinforces the idea, expressed earlier,^{2b} that the structure of the $[H_3Pt_2(\text{dppe})_2]^+$ cation is suggestive of a donor–acceptor complex, in which a neutral 16-electron $H_2Pt(\text{dppe})$ unit (around Pt(2)) acts as a donor (through two Pt–H bonds) to a cationic 14-electron $[HPt(\text{dppe})]^+$ unit (around Pt(1)).

(7) $R(F) = \sum |F_o - |F_c|| / \sum F_o$. $R_w(F) = [\sum w(F_o - |F_c|)^2 / \sum wF_o^2]^{1/2}$. $R(F^2) = \sum |F_o^2 - |F_c|^2| / \sum F_o^2$. $R_w(F^2) = [\sum w(F_o^2 - |F_c|^2)^2 / \sum wF_o^4]^{1/2}$.

(8) Because of the large number of atoms involved (154), the parameters ($n_s = 1388$) had to be divided into three blocks during least-squares refinement. The composition of the blocks was changed from cycle to cycle, and the model converged after four complete cycles of refinement so that all parameter shifts were $< 0.5\sigma$. The data-to-parameter ratio for the neutron analysis is 9.25, and the goodness of fit $S = \sum w(F_o^2 - |F_c|^2)^2 / (n_{\text{observed}} - n_s) = 1.09$. Least-squares calculations were performed with the program UPALS (Lundgren, J. O. Report UUIC-B13-4-05, University of Uppsala, 1982).

(9) For purposes of comparison, the bridging Pt–H distance in $[H_4IrPt(\text{PEt}_3)_4]^+$ is 1.73 Å, based on our recent neutron analysis (Emge, T. J.; Koetzle, T. F.; Albinati, A.; Venanzi, L. M. "American Crystallographic Association Meeting Abstracts", Columbia, MO, 1983).

The H(b1)···H(b2) nonbonding distance (2.339 (3) Å) is comparable to those found in other $M(\mu\text{-H})_2M$ fragments: 2.405 (3) Å in $[\text{H}_2\text{W}_2(\text{CO})_8]^{2-}$,¹⁰ 2.465 (14) Å in $\text{H}_2\text{Rh}_2[\text{P}(\text{O}-i\text{-Pr})_3]_4$,¹¹ and 2.376 (3) Å in $\text{H}_2\text{Os}_3(\text{CO})_{10}$.¹² These values, which were all obtained from accurate neutron diffraction analyses, seem to indicate that H···H distances in doubly bridged M–M bonds stay fairly constant at about 2.4 Å.

Finally, it should be mentioned that the present structure determination represents the most accurate measurement of a terminal Pt–H bond distance carried out to date (1.610 (2) Å). Earlier measurements (by X-ray diffraction) yielded values of 1.527,^{2b} 1.66,¹³ 1.78,¹⁴ and 1.98 Å.¹⁵

Acknowledgment. This research was supported by the Petroleum Research Fund, administered by the American Chemical Society, and by the Consiglio Nazionale delle Ri-

cherche (CNR), Rome. Work at Brookhaven National Laboratory was performed under contract with the U.S. Department of Energy. We wish to thank Dr. Thomas J. Emge, Joseph Henriques, Dr. Richard M. Kirchner, and Saeed I. Khan for assistance in parts of this work.

Registry No. $[\text{H}_3\text{Pt}_2(\text{Ph}_2\text{PCH}_2\text{CH}_2\text{PPh}_2)_2]^+[\text{BPh}_4]^-$, 88130-93-2.

Supplementary Material Available: Listings of the final atomic coordinates and anisotropic temperature factors (Table A), interatomic distances (Table B), bond angles (Table C), and average molecular parameters (Table D) for the neutron analysis (16 pages). Ordering information is given on any masthead page.

Department of Chemistry
University of Southern California
Los Angeles, California 90089

Michael Y. Chiang
Robert Bau*

Istituto di Chimica Analitica
Università di Sassari
Sassari 07100, Italy

Giovanni Minghetti*

Centro CNR
Dipartimento di Chimica Inorganica e
Metallorganica
Università di Milano
Milano 20133, Italy

Anna Laura Bandini
Guido Banditelli

Chemistry Department
Brookhaven National Laboratory
Upton, New York 11973

Thomas F. Koetzle*

Received October 14, 1983

- (10) Wei, C. Y.; Marks, M. W.; Bau, R.; Kirtley, S. W.; Bisson, D. E.; Henderson, M. E.; Koetzle, T. F. *Inorg. Chem.* **1982**, *21*, 2556.
(11) Teller, R. G.; Williams, J. M.; Koetzle, T. F.; Burch, R. R.; Gavin, R. M.; Muetterties, E. L. *Inorg. Chem.* **1981**, *20*, 1806.
(12) Broach, R. W.; Williams, J. M. *Inorg. Chem.* **1979**, *18*, 314.
(13) Kane, A. R.; Guggenberger, L. J.; Muetterties, E. L. *J. Am. Chem. Soc.* **1970**, *92*, 2571.
(14) Auburn, M.; Ciriano, M.; Howard, J. A. K.; Murray, M.; Pugh, N. J.; Spencer, J. L.; Stone, F. G. A.; Woodward, P. J. *Chem. Soc., Dalton Trans.* **1980**, 659.
(15) Furlani, A.; Licocchia, S.; Russo, M. V.; Villa, A. C.; Guastini, C. J. *Chem. Soc., Dalton Trans.* **1982**, 2449.
(16) Molecular plots were generated by the program ORTEP-II: Johnson, C. K. *Oak Ridge Natl. Lab. [Rep.]*, ORNL (U.S.) **1976**, ORNL-5138.

Articles

Contribution from the Department of Chemistry,
Texas A&M University, College Station, Texas 77843

Characterization of a Fischer–Tropsch Catalyst Prepared by Decarbonylation of Dodecacarbonyltetracobalt on Alumina

GREGORY F. MEYERS and MICHAEL B. HALL*

Received September 30, 1982

When supported on partially dehydroxylated $\gamma\text{-Al}_2\text{O}_3$, $\text{Co}_4(\text{CO})_{12}$ is an active Fischer–Tropsch (F-T) catalyst. The catalyst is deposited out of hexane solution, thermally decarbonylated, and reacted in the presence of 3:2 $\text{H}_2\text{-CO}$ at 250 °C. The zerovalent cluster, when initially deposited on the support, is extremely sensitive to oxidation. X-ray photoelectron spectroscopy (XPS) indicates that the extent of oxidation is to Co(II). XPS of the decarbonylated and used catalyst indicates the presence of reduced cobalt species in addition to Co(II). This latter observation is supported by laser-induced mass spectroscopy (LIMS). After thermal decarbonylation, the LIMS shows that cobalt clusters, Co_x ($x = 2, 5, 6, 7$), are present. After one F-T cycle, only Co_4 clusters of the type $\text{Co}_4(\text{CO})_x$ ($x = 2\text{--}6$) and cluster carbides, $\text{Co}_4(\text{CO})_xC$ ($x = 0, 1, 2, 4, 11$), are present on the surface. Under mild conditions, the catalyst after one F-T cycle cannot be completely reduced to Co(0) nor oxidized to Co(III) as evidenced by the XPS of $\text{H}_2\text{-}$ and $\text{O}_2\text{-}$ treated samples. Transmission electron microscopy (TEM) showed no visible Co particles (>10 nm) on any sample.

Currently, there is a renewed interest in the Fischer–Tropsch (F-T) synthesis^{1,2} as a potentially viable alternative to the production of gasoline and chemical feedstocks.³ Typically, the group 8 metals show the greatest specific activity for the reaction;⁴ however, these catalysts are derived from mononu-

clear salts in which the metal is initially in a relatively high oxidation state. Pretreatment of the supported metal traditionally involves high-temperature calcination and reduction, which can lead to metal sintering (and, therefore, poor dispersion).⁵ Recently, it has been demonstrated that catalysts derived from mononuclear group 6⁶ and polynuclear group 8⁷

- (1) Storch, H. H.; Golumbic, N.; Anderson, R. B. "The Fischer-Tropsch and Related Synthesis"; Wiley: New York, 1951.
(2) Masters, C. *Adv. Organomet. Chem.* **1979**, *17*, 61.
(3) (a) Haggin, J. *Chem. Eng. News* **1981**, *59* (Oct 26), 22. (b) King, R. B.; Cusumano, J. A.; Garten, R. L., *Catal. Rev.—Sci. Eng.* **1981**, *23* (1/2), 233. (c) Pruet, R. L. *Science (Washington, D.C.)* **1981**, *211*, 11.

- (4) (a) Vannice, M. A. *Adv. Chem. Ser.* **1977**, No. 163, 15. (b) Vannice, M. A. *J. Catal.* **1975**, *37*, 449.
(5) (a) Anderson, J. R. "Structure of Metallic Catalysts"; Academic Press: New York, 1975. (b) Geus, J. W. "Sintering and Catalysis"; Kucynski, G. C., Ed.; Plenum Press: New York, 1975.